$(PPh_4)[Mn_3(CO)_{12}(\mu_3\text{-}H)(\mu\text{-}Hg\{Mo(CO)_3(\eta^5\text{-}C_5H_5)\})]$: The First Example of a Mercury-Containing Planar Triangulated Rhomboidal Metal Cluster

Oriol Rossell,* Miquel Seco,* Glòria Segalés, and Santiago Alvarez

Departament de Química Inorgànica, Universitat de Barcelona, Diagonal 647, E-08028 Barcelona, Spain

Maria Angela Pellinghelli and Antonio Tiripicchio*

Istituto di Chimica Generale ed Inorganica, Università di Parma, Centro di Studio per la Strutturistica Diffrattometrica del CNR, Viale delle Scienze 78, I-43100 Parma, Italy

Received September 20, 1993®

The reaction of $(PPh_4)_2[Mn_3(CO)_{12}(\mu\text{-}H)]$ with ClHgm in tetrahydrofuran gives good yields of the new pentanuclear clusters $(PPh_4)[Mn_3(CO)_{12}(\mu_3\text{-}H)(\mu\text{-}Hg(m))]$ (m = $Mo(CO)_3Cp$ (**1a**), $W(CO)_3Cp$ (**1b**), $Mn(CO)_5$ (**1c**), $Co(CO)_4$ (**1d**), $Fe(CO)_2Cp$ (**1e**)). The structure of **1a** has been determined by X-ray diffraction methods. Crystals are triclinic, space group $P\bar{1}$ with $Z = 2$ in a unit cell of dimensions $a = 12.511(8)$ Å, $b = 13.604(9)$ Å, $c = 15.200(8)$ Å, $\alpha = 74.20(2)°$, $\beta = 70.08(2)°$, and $\gamma = 88.74(2)°$. The structure has been solved from diffractometer data by direct and Fourier methods and refined by blocked full-matrix least-squares methods on the basis of 7351 observed reflections to R and R_w values of 0.0436 and 0.0601, respectively. The structure is characterized by a roughly planar pentanuclear $MoHgMn_3$ metal core consisting of a Hg–Mn_3 triangulated rhomboidal framework with the Mo atom in plane "spiked" to the Hg atom. Although the hydride could not be located unambiguously, qualitative MO analysis indicates that it should be located inside the Mn_3Hg rhombus, probably bonded to its Mn_3 triangle. Polychlorophenyl bimetallic clusters, $(PPh_4)[Mn_3(CO)_{12}(\mu_3\text{-}H)(\mu\text{-}HgR)]$ (R = C_6Cl_5 (**3a**), 2,3,4,6-C_6HCl_4 (**3b**), 2,4,6-$C_6H_2Cl_3$ (**3c**)), were obtained as the sole isolable products by allowing the salt $(PPh_4)_2[Mn_3(CO)_{12}(\mu\text{-}H)]$ to react with ClHgR. **3a** reacts in tetrahydrofuran with 1 equiv of $[Pt(C_2H_4)(PPh_3)_2]$, affording the new insertion product $(PPh_4)[Mn_3(CO)_{12}(\mu_3\text{-}H)(\mu\text{-}Hg\{Pt(C_6Cl_5)(PPh_3)_2\})]$ (**4**), which represents a new class of Hg–Pt–R insertion reaction.

Introduction

The chemistry of mercury-containing transition-metal clusters is of current interest[1] and, in particular, clusters containing mercury atoms of coordination number greater than 2 are being intensively investigated. One interesting class of such species includes those resulting from the interaction between a mercury and a M_3 metal triangle. For this metal system, three possible geometries can be anticipated:

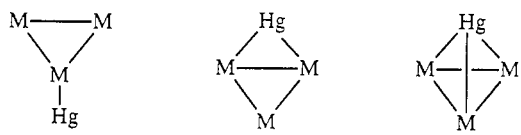

A shows a "terminal" mercury linkage with a two-center two-electron transition metal–mercury bond; **B** represents an edge-bridged linkage with a three-center two-electron mercury–transition metal bond, and in **C** the mercury atom appears capping the M_3 metal face. Although no examples of **A** have been reported, **B** and **C** are well represented in the literature.[2,3] Interestingly, when the formally two-coordinate μ_2-HgX moiety (X = halide or a metal fragment, such as $Mo(CO)_3Cp$) bridges an M–M edge (case **B**), the resulting metal skeleton invariably consists of a butterfly arrangement with dihedral angles between the M_3 and M_2Hg planes ranging from 112[2d] to 132°.[2e]

In this paper we describe the first example of a mercury-containing planar triangulated rhombohedral metal cluster, $(PPh_4)[Mn_3(CO)_{12}(\mu_3\text{-}H)(\mu\text{-}Hg\{Mo(CO)_3Cp\})]$ (Cp = η^5-C_5H_5), which has been structurally chacterized by an X-ray study. The stability of this derivative, as well as other similar derivatives with different metal fragments or containing polychlorophenyl groups bonded to the mercury atom toward redistribution processes is discussed.

® Abstract published in *Advance ACS Abstracts*, February 1, 1994.

(1) An excellent review on mercury–transition metal clusters has just been published: Gade, L. M. *Angew. Chem., Int. Ed. Engl.* **1993**, *32*, 24.

(2) (a) King, K.; Rosenberg, E.; Tiripicchio, A.; Tiripicchio-Camellini, M. *J. Am. Chem. Soc.* **1980**, *102*, 3626. (b) Rosenberg, E.; Hardcastle, K. I.; Tiripicchio, A.; Tiripicchio-Camellini, M.; Ermer, S. E.; King, K. *Inorg. Chem.* **1983**, *22*, 1339. (c) Rosenberg, E.; Ryckman, D.; Gellert, R. W.; Hsu, I. *Inorg. Chem.* **1986**, *25*, 194. (d) Rosenberg, E.; Hardcastle, K. I.; Day, M. W.; Gobetto, R. *Organometallics* **1991**, *10*, 203. (e) Andreu, P. L.; Cabeza, J. A.; Llamazares, A.; Riera, V.; Bois, C.; Jeanin, Y. *J. Organomet. Chem.* **1991**, *420*, 431. (f) Andreu, P. L.; Cabeza, J. A.; Llamazares, A.; Riera, V.; Garcia-Granda, S.; Van der Maelen, J. F. *J. Organomet. Chem.* **1992**, *434*, 123.

(3) (a) Horwitz, P.; Holt, E. M.; Brock, C. P.; Shriver, D. F. *J. Am. Chem. Soc.* **1985**, *107*, 8136. (b) Wang, M.; Sabat, M.; Horwitz, C. P.; Shriver, D. F. *Inorg. Chem.* **1988**, *27*, 552. (c) Mednikov, E. G.; Bashilov, V. V.; Sokolov, V. I.; Slovokhotov, Yu, T.; Struchkov, Yu. T. *Polyhedron* **1983**, *2*, 141. (d) Mednikov, E. G.; Eremenko, N. K.; Bashilov, V. V.; Sokolov, V. I. *Inorg. Chim. Acta* **1983**, *76*, L31. (e) Braunstein, P.; Rosé, J.; Tiripicchio, A.; Tiripicchio Camellini, M. *J. Chem. Soc., Chem. Commun.* **1984**, 391. (f) Henly, T. J.; Shapley, J. R. *Organometallics* **1989**, *8*, 2729. (g) Braunstein, P.; Rosé, J.; Tiripicchio, A.; Tiripicchio-Camellini, M. *J. Chem. Soc.* **1992**, 911. (h) Bianchini, A.; Farrugia, L. J. *Organometallics* **1992**, *11*, 540.

0276-7333/94/2313-2205$04.50/0

Finally, the insertion of the carbene-like $Pt(PPh_3)_2$ fragment into the Hg–C bond of $(PPh_4)[Mn_3(CO)_{12}(\mu_3\text{-}H)\{\mu\text{-}Hg(C_6Cl_5)\}]$ to give the pentanuclear $(PPh_4)[Mn_3(CO)_{12}(\mu_3\text{-}H)(\mu\text{-}Hg\{Pt(C_6Cl_5)(PPh_3)_2\})]$ cluster is also reported.

Results

The reaction of ClHg(m) (m = metal fragment) with $(PPh_4)_2[Mn_3(CO)_{12}(\mu\text{-}H)]$ in THF at −15 °C affords good yields of the dark green complex $(PPh_4)[Mn_3(CO)_{12}(\mu_3\text{-}H)(\mu\text{-}Hg(m))]$ (m = $Mo(CO)_3Cp$ (**1a**), $W(CO)_3Cp$ (**1b**), $Mn(CO)_5$ (**1c**), $Co(CO)_4$ (**1d**), $Fe(CO)_2Cp$ (**1e**)) as a result of electrophilic attack of the $Hg(m)^+$ fragment at the metal–metal bond (eq 1).

$$[Mn_3(CO)_{12}(\mu\text{-}H)]^{2-} + ClHg\text{-}m \longrightarrow$$

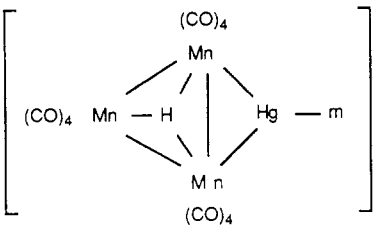

(1)

1a–e are air-stable solids, but their THF solutions decompose slowly under nitrogen at room temperature. They were characterized by elemental analyses and spectroscopic techniques. The $\nu(CO)$ IR pattern is almost identical for all of them, showing along with the bands due to the m units, bands of the "$Mn_3(CO)_{12}(\mu\text{-}H)$" fragment slightly shifted to higher frequencies relative to the starting $[Mn_3(CO)_{12}(\mu\text{-}H)]^{2-}$ anion (see Experimental Section). The ^1H NMR spectra are not very informative but in all cases show the presence of the hydride ligand at about −21.5 ppm. The FAB(−) mass spectra of the negative ions of **1a–e** were recorded using NBA as the matrix, and the patterns in all these spectra are very similar. They show the parent molecular ion in relatively high abundance along with the $[HMn_3(CO)_{12}HgMn(CO)_5]^-$ fragment that invariably appears in all of them. The exact nature of the resulting compounds was deduced by the X-ray study of **1a**.

Polychlorophenyl mercury/manganese clusters, $(PPh_4)[Mn_3(CO)_{12}(\mu_3\text{-}H)(\mu\text{-}HgR)]$ (R = C_6Cl_5 (**3a**), 2,3,4,6-C_6HCl_4 (**3b**), 2,4,6-$C_6H_2Cl_3$ (**3c**)), were obtained in good yields, as the sole isolable products, by a similar reaction between the halide polychlorophenyl mercury compounds, ClHgR, and the salt $(PPh_4)_2[Mn_3(CO)_{12}(\mu\text{-}H)]$ in THF solution. **3a–c** are soluble in THF and CH_2Cl_2, but sparingly soluble in toluene or hexane. $(PPh_4)[Mn_3(CO)_{12}(\mu_3\text{-}H)(\mu\text{-}HgR)]$ (R = Ph, 2,3,4,5-C_6HCl_4) were obtained contaminated by $(PPh_4)_2[\{Mn_3(CO)_{12}(\mu_3\text{-}H)\}_2(\mu_4\text{-}Hg)]$ (**2**) as a result of redistribution reactions, and no attempt was made to separate both products. **2** was also synthesized in high yields by the reaction of $Hg(NO_3)_2$ or $Hg(CN)_2$ with $(PPh_4)_2[Mn_3(CO)_{12}(\mu\text{-}H)]$ in THF in a 1:2 molar ratio. The mixed Pt/Mn/Hg cluster, $(PPh_4)[Mn_3(CO)_{12}(\mu_3\text{-}H)(\mu\text{-}Hg\{Pt(C_6Cl_5)(PPh_3)_2\})]$ was formed by allowing $(PPh_4)[Mn_3(CO)_{12}(\mu_3\text{-}H)\{\mu\text{-}Hg(C_6Cl_5)\}]$ to react with the zerovalent platinum complex $[Pt(C_2H_4)(PPh_3)_2]$ in THF at 30 °C. This cluster was moderately stable in THF solutions under nitrogen, and it could be manipulated as a solid in the air for several minutes.

Discussion

One interesting feature of these new metal clusters is their stability toward metal ligand redistribution reactions. There are many reports concerning the reaction represented in eq 2, and it is generally assumed that while most

$$2L_pM_q\text{–}HgX \rightarrow L_pM_q\text{–}Hg\text{–}M_qL_p + HgX_2 \quad (2)$$

of the two-center two-electron bonded transition-metal mercury compounds redistribute to unsymmetric species,[4] complexes containing two-coordinate μ_2-HgX moieties (X = halide or metal fragment) bridging an M–M edge favor the formation of symmetric species, particularly at high temperature.[5] A possible explanation of this behavior is that the probable pathway for the redistribution reactions involves a bimolecular, associative process, believed to proceed through a four-center bridged transition state,[6] which is unlikely for complexes containing mercury atoms which are four-coordinate or more. It is worth noting that such a mechanism would require of mercury greater coordination numbers than those usually observed for this metal. In addition, we have recently reported, in support of this idea, that anionic metal clusters are by far much less disposed to undergo symmetrization reactions than the neutral compounds. Thus the reluctance of the anionic spiked triangle clusters $[Fe_2(CO)_6(\mu\text{-}CO)_2(\mu\text{-}Hg(m))]^-$ to give the spiro $[\{Fe_2(CO)_8\}_2Hg]^{2-}$ metal cluster as compared with the highly unstable neutral $[Fe_2(CO)_6(\mu\text{-}CO)(\mu\text{-}PPh_2)(\mu\text{-}Hg(m))]$ derivative is noticeable.[7]

With this in mind, and with the object to gain insight into the metal ligand redistribution reactions for metal clusters of higher nuclearity, we undertook the present study allowing the dianion $[Mn_3(CO)_{12}(\mu\text{-}H)]^{2-}$ to react with ClHgm. According to the ideas above, it could be anticipated that stable metal clusters $[Mn_3(CO)_{12}(\mu_3\text{-}H)(\mu\text{-}Hgm)]^-$ would be formed. This is because the delocalized negative charge over the derivative could hinder the approach of two species, thus precluding the redistribution of the metal ligands. In a separate reaction, $Hg(NO_3)_2$ or $Hg(CN)_2$ were reacted with $[Mn_3(CO)_{12}(\mu\text{-}H)]^{2-}$ in a 1:2 molar ratio in an attempt to synthesize and characterize the spiro complex $(PPh_4)_2[\{Mn_3(CO)_{12}(\mu_3\text{-}H)\}_2(\mu_4\text{-}Hg)]$ (**2**) which showed a characteristic band at 2045 cm^{-1} in the IR spectrum. Pure $(PPh_4)[Mn_3(CO)_{12}(\mu_3\text{-}H)(\mu\text{-}Hg(m))]$ was prepared, free of the band at 2045 cm^{-1}, in good yields, showing that no redistribution process had occurred. Only after reaching room temperature did solutions of **1a–e** begin to show the band at 2045 cm^{-1} along with others resulting from the partial decomposition of the products. These results support the hypothesis that the negative charge on the metals precludes the symmetrization process, according to the bimolecular mechanism proposed.

The nucleophilicity of the new clusters was low and, thus, they did not react with 1 equiv of $ClAuPR_3$ (R = Ph or Me) to yield the mixed tetrametallic Mn/Hg/Mo/Au

(4) (a) Mays, M. J.; Robb, J. D. *J. Chem. Soc. A* **1968**, 329. (b) Glockling, F.; Mahale, V. B.; Sweeney, J. *J. Chem. Soc., Dalton Trans.* **1979**, 767. (c) Rossell, O.; Seco, M.; Torra, I. *J. Chem. Soc., Dalton Trans.* **1986**, 1011.

(5) (a) Iggo, J. A.; Mays, M. *J. Chem. Soc., Dalton Trans.* **1984**, 643. (b) Rosenberg, E.; Rickman, D.; I-Nan Hsu; Gellert, R. W. *Inorg. Chem.* **1986**, *25*, 194.

(6) Abraham, M. H. In *Comprehensive Chemical Kinetics*; Bamford, C. H., Tipper, C. F. H., Eds.; Elsevier: Amsterdam, 1973; Vol. 12.

(7) Reina, R.; Rossell, O.; Seco, M. *J. Organomet. Chem.* **1990**, *398*, 285.

hexanuclear species $[Mn_3(CO)_{12}(\mu_3\text{-}H)(\mu\text{-}Hg\{Mo(CO)_3Cp\})(\mu\text{-}AuPR_3)]$, probably due to the steric constrains of ligands. The decrease in the nucleophilicity of the dinegative metal cluster when a metal fragment is incorporated has been described for other metal systems[8] and may be explained on the basis of steric arguments.

These results prompted us to try the synthesis of analogous polychlorophenyl mercury salts $(PPh_4)[Mn_3(CO)_{12}(\mu_3\text{-}H)(\mu\text{-}HgR)]$, since these could be interesting precursors of the mixed platinum/manganese/mercury derivatives, $(PPh_4)[Mn_3(CO)_{12}(\mu_3\text{-}H)(\mu\text{-}Hg\{PtR(PPh_3)_2\})]$, considering that the $Pt(PPh_3)_2$ fragment easily inserts into the Hg–C bond.[9] These derivatives were prepared by reaction of the manganese anion with ClHgR (R = C_6Cl_5, 2,3,4,6-C_6HCl_4, 2,4,6-$C_6H_2Cl_3$). Remarkably, for R containing no chlorine (R = Ph) or only one chlorine atom in the ortho position relative to the Hg–C bond (R = 2,3,4,5-C_6HCl_4), an extensive ligand redistribution took place to yield $[(\mu_4\text{-}Hg)\{Mn_3(CO)_{12}(\mu_3\text{-}H)\}_2]^{2-}$, in spite of the negative charge of the cluster. A similar effect had been described earlier for some bimetallic Mo- or W–mercury complexes, $[Cp(CO)_3M\text{–}HgR]$.[10] This behavior shows not only that the negative charge has an important role in symmetrization reactions but also that the volume or steric congestion of ligands attached to the metal centers should be considered.

Because of the high stability toward the symmetrization, the potential use of complex **3a** as a precursor to platinum-containing derivatives was studied. Reaction between **3a** and $[Pt(C_2H_4)(PPh_3)_2]$ was carried out in THF at 30 °C and monitored by ^{31}P NMR spectroscopy. After 2 h, two main peaks at 60.1 (P_A) and 18.2 ppm (P_B) (relative to H_3PO_4) with the corresponding platinum satellites, $J(P_A\text{–}^{195}Pt)$ = 2406 Hz and $J(P_B\text{–}^{195}Pt)$ = 2876 Hz, showed a cis platinum–phosphine insertion to give $(PPh_4)[Mn_3(CO)_{12}(\mu_3\text{-}H)(\mu\text{-}Hg\{Pt(C_6Cl_5)(PPh_3)_2\})]$ (**4**) similar to that observed in the reactions between platinum(0) complexes and $[(PPh_3)_2(C_6Cl_5)Pt\text{-}Hg(C_6Cl_5)]$[11] and $[Cp(CO)_3M\text{–}Hg(C_6Cl_5)]$ (M = Mo, W).[9b]

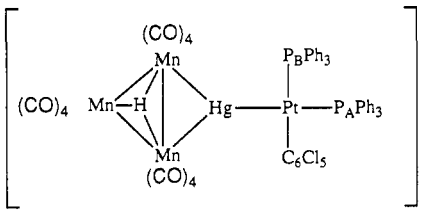

Mercury satellites were only seen for P_A ($^2J(P_A\text{–}^{199}Hg)$ = 2960 Hz) whereas those corresponding to P_B were obscured by other signals. It is interesting that the coupling constant, $J(^{31}P_A\text{–}^{195}Pt)$ for **4** is smaller than those found for the series $[(PPh_3)_2RPt\text{–}HgR]$[12] and $[Cp(CO)_3M\text{–}Hg\text{–}Pt(C_6Cl_5)(PPh_3)_2]$[9b] (in the range between 2630 and 2850 Hz). This finding[13] suggests a decrease in the trans influence on going from HgR to $[Hg\{M(CO)_3Cp\}]$ and finally to $[Hg\{Mn_3(CO)_{12}(\mu\text{-}H)\}_2]$. On the other hand, the coupling constant $^2J(P\text{–}^{199}Hg)$ is in the expected range for this class of derivatives.[9b] It should be noted that, despite the long reaction time and the relatively high temperatures, no symmetrization process occurred, and the resulting pentanuclear cluster could be isolated in analytically pure form.

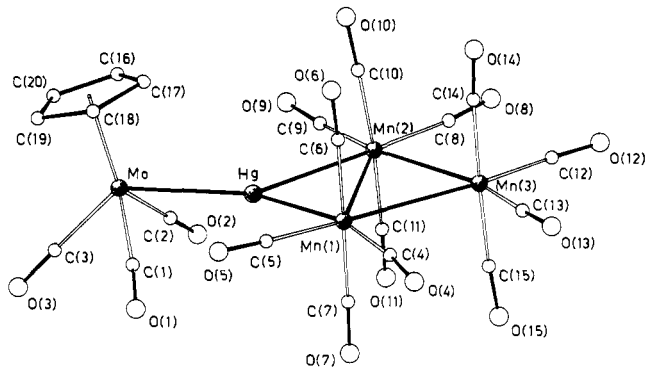

Figure 1. View of the molecular structure of the anion $[Mn_3(CO)_{12}(\mu_3\text{-}H)(\mu\text{-}Hg\{Mo(CO)_3Cp\})]^-$ (**1a**) together with the atomic numbering scheme.

Crystal Structure of 1a. The structure of the anion of **1a** is shown in Figure 1 together with the atomic numbering scheme. Selected bond distances and angles are given in Table 1. The structure is characterized by a roughly planar pentanuclear $MoHgMn_3$ metal core consisting of a $Hg\text{–}Mn_3$ triangulated rhomboidal framework with the Mo atom in plane "spiked" to the Hg atom. The dihedral angle between the two HgMn(1)Mn(2) and Mn(1)Mn(2)Mn(3) triangles is 3.8(1)° with the Hg atom deviating by 0.147(1) Å from the Mn(1)Mn(2)Mn(3) triangle. The mercury atom shows an approximately trigonal coordination, involving the Mn(1), Mn(2), and Mo atoms. The $CpMo(CO)_3Hg$ moiety shows the usual "four legged piano-stool" arrangement with the Mo–Hg distance of 2.790(2) Å. The ligand shell of the Mn_3 fragment cluster is completed by twelve carbonyl ligands, six in equatorial positions (four trans to the manganese atom and two trans to the mercury metal) and six in axial positions. The hydride could not be located, but an indirect location by means of a "potential energy" technique and theoretical calculations was carried out.

A comparison of the structure of **1a** with that of the starting anion $[Mn_3(CO)_{12}(\mu\text{-}H)]^{2-}$ reveals that the presence of the $HgMo(CO)_3Cp$ group in **1a** results in a lengthening of all the Mn–Mn distances, and particularly that corresponding to the edge-bridged Mn(1)–Mn(2).[14] This enlarging effect on the incorporation of proton-isolobal metal fragments, such as HgR^+ or $AuPPh_3^+$, in mono- or dianions is well established and explanations

(8) Rossell, O.; Seco, M.; Jones, P. G. *Inorg. Chem.* **1990**, *29*, 348. (b) Alvarez, S.; Rossell, O.; Seco, M.; Valls, J.; Pellinghelli, M. A.; Tiripicchio, A. *Organometallics* **1991**, *10*, 2309.

(9) See for example: (a) Sokolov, V. I.; Reutov, O. A. *Coord. Chem. Rev.* **1978**, *27*, 89. (b) Braunstein, P.; Rossell, O.; Seco, M.; Torra, I.; Solans, X.; Miravitlles, C. *Organometallics*, **1986**, *5*, 1113.

(10) Rossell, O.; Seco, M.; Braunstein, P. *J. Organomet. Chem.* **1984**, *273*, 233.

(11) Rossell, O.; Seco, M.; Torra, I.; Solans, X.; Font-Altaba, M. *J. Organomet. Chem.* **1984**, *270*, C63.

(12) Rossell, O.; Sales, J.; Seco, M. *J. Organomet. Chem.* **1982**, *236*, 415.

(13) Allen, F. H.; Pidcock, A.; Watherhouse, C. R. *J. Chem. Soc. A* **1970**, 2087.

(14) Schatz, W.; Neumann, H. P.; Nuber, B.; Kanellakopulos, B.; Ziegler, M. L. *Chem. Ber.* **1991**, *124*, 453.

Table 1. Selected Bond Distances (Å) and Angles (deg) with Esd's in Parentheses for Compound 1a

Hg–Mo	2.790(2)	Mn(3)–C(13)	1.783(11)
Hg–Mn(1)	2.698(2)	Mn(3)–C(14)	1.852(9)
Hg–Mn(2)	2.713(2)	Mn(3)–C(15)	1.838(7)
Mn(1)–Mn(2)	3.142(2)	C(1)–O(1)	1.144(11)
Mn(1)–Mn(3)	2.944(2)	C(2)–O(2)	1.170(10)
Mn(2)–Mn(3)	2.955(2)	C(3)–O(3)	1.142(11)
Mo–C(1)	1.979(9)	C(4)–O(4)	1.153(10)
Mo–C(2)	1.962(7)	C(5)–O(5)	1.159(12)
Mo–C(3)	1.973(8)	C(6)–O(6)	1.135(8)
Mo–CE[a]	2.006(7)	C(7)–O(7)	1.141(8)
Mn(1)–C(4)	1.795(8)	C(8)–O(8)	1.136(13)
Mn(1)–C(5)	1.786(9)	C(9)–O(9)	1.160(14)
Mn(1)–C(6)	1.847(6)	C(10)–O(10)	1.165(9)
Mn(1)–C(7)	1.837(7)	C(11)–O(11)	1.154(10)
Mn(2)–C(8)	1.812(10)	C(12)–O(12)	1.159(12)
Mn(2)–C(9)	1.788(10)	C(13)–O(13)	1.160(16)
Mn(2)–C(10)	1.825(8)	C(14)–O(14)	1.115(11)
Mn(2)–C(11)	1.829(7)	C(15)–O(15)	1.127(9)
Mn(3)–C(12)	1.792(9)		

Mo–Hg–Mn(1)	147.68(4)	Mn(3)–Mn(2)–C(10)	92.4(3)
Mo–Hg–Mn(2)	140.41(4)	Mn(3)–Mn(2)–C(11)	92.0(3)
Mn(1)–Hg–Mn(2)	71.00(4)	C(8)–Mn(2)–C(9)	94.2(4)
Hg–Mn(1)–Mn(2)	54.73(3)	C(8)–Mn(2)–C(10)	93.2(5)
Hg–Mn(2)–Mn(1)	54.27(3)	C(8)–Mn(2)–C(11)	89.7(5)
Mn(2)–Mn(1)–Mn(3)	57.97(4)	C(9)–Mn(2)–C(10)	87.3(4)
Mn(1)–Mn(2)–Mn(3)	57.65(4)	C(9)–Mn(2)–C(11)	88.6(4)
Mn(1)–Mn(3)–Mn(2)	64.37(4)	Mn(1)–Mn(3)–C(13)	98.8(3)
Hg–Mo–CE	105.8(3)	Mn(1)–Mn(3)–C(14)	93.6(3)
Hg–Mo–C(1)	70.9(3)	Mn(1)–Mn(3)–C(15)	88.4(3)
Hg–Mo–C(2)	71.7(2)	Mn(2)–Mn(3)–C(12)	100.4(3)
Hg–Mo–C(3)	134.9(2)	Mn(2)–Mn(3)–C(14)	89.7(3)
CE–Mo–C(1)	127.9(4)	Mn(2)–Mn(3)–C(15)	91.7(3)
CE–Mo–C(2)	129.8(3)	C(12)–Mn(3)–C(13)	96.5(4)
CE–Mo–C(3)	119.3(3)	C(12)–Mn(3)–C(14)	89.5(4)
C(1)–Mo–C(2)	99.4(3)	C(12)–Mn(3)–C(15)	88.8(4)
C(1)–Mo–C(3)	80.4(4)	C(13)–Mn(3)–C(14)	89.5(4)
C(2)–Mo–C(3)	79.9(3)	C(13)–Mn(3)–C(15)	89.5(4)
Hg–Mn(1)–C(5)	76.4(3)	Mo–C(1)–O(1)	174.5(8)
Hg–Mn(1)–C(6)	94.7(2)	Mo–C(2)–O(2)	176.1(6)
Hg–Mn(1)–C(7)	83.4(2)	Mo–C(3)–O(3)	178.5(7)
Mn(3)–Mn(1)–C(4)	79.7(2)	Mn(1)–C(4)–O(4)	172.3(7)
Mn(3)–Mn(1)–C(6)	86.9(2)	Mn(1)–C(5)–O(5)	173.3(9)
Mn(3)–Mn(1)–C(7)	93.8(2)	Mn(1)–C(6)–O(6)	175.4(6)
C(4)–Mn(1)–C(5)	92.0(4)	Mn(1)–C(7)–O(7)	176.9(7)
C(4)–Mn(1)–C(6)	92.7(3)	Mn(2)–C(8)–O(8)	172.7(9)
C(4)–Mn(1)–C(7)	89.2(3)	Mn(2)–C(9)–O(9)	176.0(8)
C(5)–Mn(1)–C(6)	87.6(4)	Mn(2)–C(10)–O(10)	175.3(8)
C(5)–Mn(1)–C(7)	91.9(4)	Mn(2)–C(11)–O(11)	176.0(7)
Hg–Mn(2)–C(9)	76.9(3)	Mn(3)–C(12)–O(12)	177.3(9)
Hg–Mn(2)–C(10)	90.3(3)	Mn(3)–C(13)–O(13)	177.8(9)
Hg–Mn(2)–C(11)	86.2(3)	Mn(3)–C(14)–O(14)	173.9(9)
Mn(3)–Mn(2)–C(8)	77.2(3)	Mn(3)–C(15)–O(15)	176.4(7)

[a] CE is the centroid of the C(16)···C(20) cyclopentadienyl ring.

based on steric arguments have been invoked.[15] The distances Hg–Mn, 2.698(2) and 2.713(2) Å, are longer than for a Hg–Mn single bond, and correspond to a three-center two-electron bond. They are also longer than the distances Mn–Hg found when a Mn atom is μ-bonded at a Hg_2 edge. It is interesting to note that we have not found in the literature any distance for a Hg atom μ-bonded at a Mn–Mn edge.

In conclusion, the structure of **1a**, showing a spiked planar triangulated rhombohedral tetrametallic framework, represents a new structural type of mercury clusters. Although rarely encountered, other metals, such as Pd or Pt,[16] have sometimes displayed this type of structure. All these facts prompted us to examine the electronic structure and chemical bonding of this new metal system.

(15) Iggo, J. A.; Mays, M. J.; Raithby, P. R.; Henrick, K. *J. Chem. Soc., Dalton Trans.* **1984**, 633.

(16) (a) Bender, R.; Braunstein, P.; Jud, J. M.; Dusausoy, Y. *Inorg. Chem.* **1983**, *22*, 3394. (b) Bender, R.; Braunstein, P.; Jud, J. M.; Dusausoy, Y. *Inorg. Chem.* **1984**, *23*, 4489.

Molecular Orbitals of a Symmetric $Mn_3(CO)_{12}$ Core. For the study of bonding and structure in $[Mn_3(CO)_{12}(\mu_3\text{-H})(\mu\text{-Hg}\{Mo(CO)_3Cp\})]^-$, we used extended Hückel molecular orbital calculations[17] on the model compound $[Mn_3(CO)_{12}(\mu\text{-H})(\mu\text{-HgCl})]^-$, in which the m^- fragment is replaced by a two-electron donor. In order to make things clearer, we start with a hypothetical and symmetric anionic cluster $[Mn_3(CO)_{12}]^{3-}$ (**D**), isoelectronic

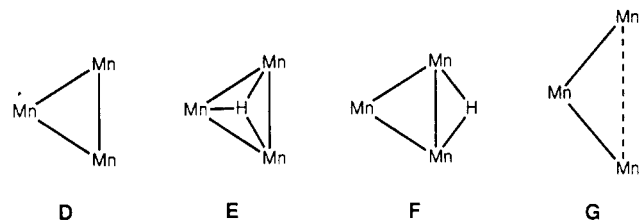

with $[Fe_3(CO)_{12}]$. Then we study its interaction with a Lewis acid, H^+, in two different isomers of the known compound[14] $[HMn_3(CO)_{12}]^{2-}$: μ_3-symmetrically bridged (**E**) or edge-bridging (**F**). The next logical step is the study of the effect of asymmetrization of the Mn_3 triangle (**G**) on the electronic structure and energy of the cluster. Finally, we undertake the study of the electronic structure of $[Mn_3(CO)_{12}(\mu\text{-HgCl})]^{2-}$ in order to establish a likely localization for an attached H^+, according to the distribution of the electron density of the frontier orbitals.

The reason for building up the structure of the model cluster stepwise is that we pursue a molecular orbital description of the Mn–Mn and Mn–X (X = H or Hg) bonds which could adequately account for the differences in Mn–Mn distances found in $[HMn_3(CO)_{12}]^{2-}$ (2.755, 2.833, and 2.881 Å),[14] $[H_3Mn_3(CO)_{12}]$ (3.099, 3.107, and 3.126 Å),[18] and $[HMn_3(CO)_{12}HgMo(CO)_3Cp]^-$ (2.955, 2.944, and 3.142 Å).

We can imagine the $[Mn_3(CO)_{12}]^{3-}$ cluster to be formed by joining three $Mn(CO)_4^-$ fragments. From the corresponding fragment molecular orbitals,[19] we need consider only those spanning the two vacant cis positions of an idealized octahedral complex ML_6. These are presented in a schematic form in Figure 2 and labeled as the atomic orbital with the largest contribution. The frontier molecular orbitals of the hypothetical cluster **D** are just the combinations of sp and xy, as shown in Figure 3, where the labels correspond to the symmetry representations of the D_{3h} point group: **D**-a_1 and **D**-1e are bonding, **D**-a_2 and **D**-2e are antibonding combinations.

The combinations of the $x^2 - y^2$ orbitals, remnants of the t_{2g} set of Mn in an octahedral ligand field, are essentially Mn–Mn nonbonding. The total calculated Mn–Mn overlap population for **D** is 0.034 per Mn–Mn bond and turns out to be negative when the three HOMO's are emptied. This means that all of the Mn–Mn bonding should be ascribed to the a_1 and e molecular orbitals.

(17) All EH molecular orbital calculations were carried out using the modified Wolfsberg-Helmholz formula for the nondiagonal H_{ij} elements. The diagonal H_{ii} elements and Slater exponents and coefficients were taken from the literature. For C, O, H: Hoffmann, R. *J. Chem. Phys.* **1963**, *39*, 1397. Ammeter, J. H.; Bürgi, H. B.; Thibeault, J. C.; Hoffmann, R. *J. Am. Chem. Soc.* **1978**, *100*, 3686. For Hg: Underwood, D. J.; Hoffmann, R.; Tatsumi, K.; Nakamura, A.; Yamamoto, Y. *J. Am. Chem. Soc.* **1985**, *107*, 5968. For Cl: Hoffmann, R.; Chen, M. M. L.; Elian, M.; Rossi, A. R.; Mingos, D. M. P. *Inorg. Chem.* **1974**, *13*, 2666. For Mn: Elian, M.; Hoffmann, R. *Inorg. Chem.* **1975**, *14*, 1058.

(18) Kirtley, S. W.; Olsen, J. P.; Bau, R. *J. Am. Chem. Soc.* **1973**, *95*, 4532.

(19) Albright, T.; Burdett, J. K.; Whangbo, M.-W. *Orbital Interactions in Chemistry*; J. Wiley: New York, 1985; p 358.

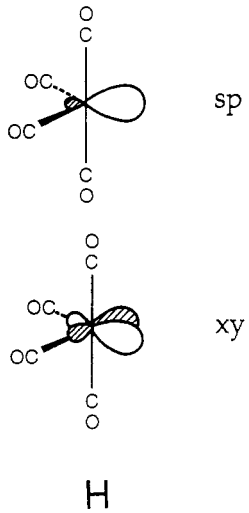

Figure 2. $Mn(CO)_4$ fragment molecular orbitals spanning the two vacant cis positions of an idealized octahedral complex ML_6.

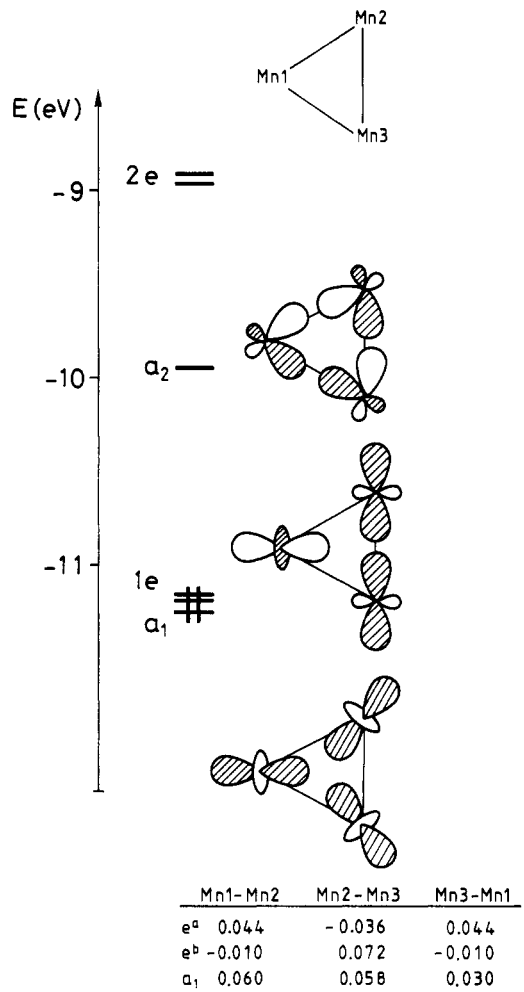

	Mn1-Mn2	Mn2-Mn3	Mn3-Mn1
e^a	0.044	-0.036	0.044
e^b	-0.010	0.072	-0.010
a_1	0.060	0.058	0.030

Figure 3. Frontier molecular orbitals of a symmetric $[Mn_3(CO)_{12}]^{3-}$ cluster. The inset shows the contributions of the different molecular orbitals to the Mn–Mn overlap populations.

If a proton is to be added to **D**, where is it more likely to sit? In the middle of the Mn_3 triangle as in **E** or bridging one of the edges as in **F**? We rule out out-of-plane geometries since the electron density of the frontier orbitals is maximum in the plane of the Mn_3 triangle. Geometry **E** can be accomplished by interacting the hydrogen 1s orbital with **D**-a_1; geometry **F**, by interaction with one of the **D**-1e orbitals. Therefore, both isomers seem to be possible, although the calculations predict **E** to be barely 0.5 eV more stable. Since total energies calculated at the EH level may not be fully reliable, especially when comparing compounds with different numbers of short interatomic distances, we prefer to look at bond strengths. The calculated OP's are shown in **I**–**K** and indicate that

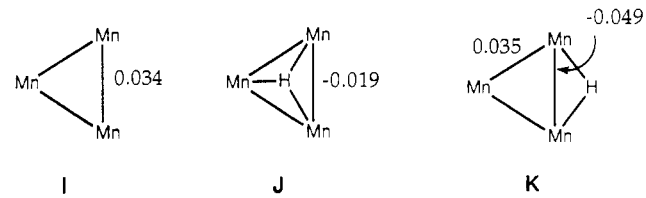

the μ_3 geometry (**E**) equally weakens all three Mn–Mn bonds relative to the hypothetical cluster **D**. On the contrary, the μ_2 isomer strongly weakens the bridged Mn–Mn bond but does not affect the unbridged ones. Bridging of another edge with an additional proton has a similar result: only the corresponding edge is affected by the resulting hydrido bridge. Similar results were reported by Mitchell and Welch[20] for the analogous rhenium clusters, $[Re_3H(CO)_{12}]^{2-}$ and $[Re_3H_2(CO)_{12}]^{-}$. Finally, in the compound with three hydrido bridges all Mn–Mn bonds are strongly weakened (Mn–Mn overlap populations = –0.047 electrons/bond), a result which is consistent with the fact that the triply bridged cluster (hydrogen atoms located in the X-ray crystal structure) $[H_3Mn_3(CO)_{12}]$ (**L**) presents longer distances in the bridged Mn–Mn edges than $[HMn_3(CO)_{12}]^{2-}$. The Mn–Mn bond distances in the latter cluster, for which the hydrogen atom has not been located, are quite similar for all three edges and shorter than in the triply bridged cluster. According to these results, the Mn–Mn bond distances in $[HMn_3(CO)_{12}]^{2-}$ are consistent with a structure of type **E**.

The above results also suggests that in the present compound, $[Mn_3(CO)_{12}(\mu_3\text{-}H)(\mu\text{-}Hg\{Mo(CO)_3Cp\})]^-$, the hydrido ligand is sitting in the middle of either the Mn_3 or the Mn_2Hg triangles. If the hydrido ligand were bridging one of the remaining Mn–Mn edges, a strong asymmetry should appear, in contradiction with the structural data (Mn–Mn = 2.944 and 2.955 Å). Such a geometry is also precluded by the orientation of the equatorial carbonyl ligands discussed in the structural section.

Asymmetrization of the Mn_3 Triangle and Interaction with Hg-X^+. In the structure of $[Mn_3(CO)_{12}(\mu_3\text{-}H)(\mu\text{-}Hg\{Mo(CO)_3Cp\})]^-$ the Mn_3 triangle is clearly asymmetric, as shown schematically in **G**. Consequently, we must analyze the effects of such asymmetrization on the electronic structure of the Mn_3 core before discussing the electronic structure of the full cluster. The effect of stretching on the Mn–Mn bonds and the simultaneous reorientation of the carbonyl groups in the hypothetical cluster $[Mn_3(CO)_{12}]^{3-}$ on its highest occupied molecular orbitals is shown in Figure 4. The e orbitals lose their degeneracy: one of them (labeled **G**-$2a_1$ in the C_{2v} point group) is somewhat destabilized (by 0.2 eV) and reoriented by symmetry allowed mixing in of the **G**-$1a_1$ orbital. This has two obvious consequences: (a) the cluster is destabilized with respect to the undistorted one, and (b) the

(20) Mitchell, G. F.; Welch, A. J. *J. Chem. Soc., Dalton Trans.* **1987**, 1017.

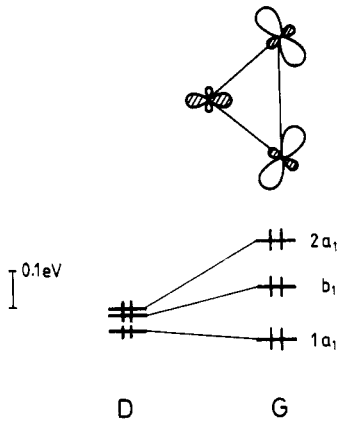

Figure 4. Splitting of the highest occupied orbitals of the $[Mn_3(CO)_{12}]^{3-}$ cluster (**D**) upon asymmetrization (**G**). The sketched molecular orbital is **G**-2a_1, one of the degenerate **D**-e set in the symmetric structure.

G-2a_1 orbital has the right topology to interact with an edge-bridging proton.

Another consequence of the asymmetrization is related to the strength of the Mn–Mn bonds and needs a more detailed discussion. The Mn–Mn overlap populations change with the asymmetrization (see **I** and **M**): the

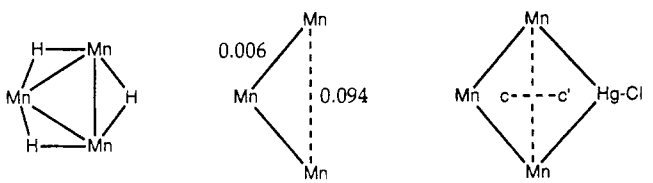

stretched bond appears to become stronger while the untouched ones are weakened. This counterintuitive behavior can be understood if one recalls that there are changes in the relative orientation of the $Mn(CO)_4$ fragments (**H**) simultaneous to the bond stretching; the decrease in Mn–Mn bonding interaction produced by elongation of the bond is recovered by reorientation of the equatorial carbonyl groups. Consequently, the Mn–Mn overlap populations of the long and short edges can no longer be expected to be clearly correlated with bond distances.

Let us see now what happens when an H^+ ion is introduced in the distorted core. The calculated energy is lower for the edge-bridging geometry than for the center-of-triangle one by 0.5 eV, due to the topological reorientation of **G**-2a_1 (Figure 4). The calculated net charge on the hydrogen atom is −0.22 in the central position and −0.27 in the edge-bridging geometry, indicating a clear hydride character in both cases, comparable to that of a bridging hydride in the $[Mo_2(CO)_8(\mu\text{-dppm})(\mu\text{-H})]^-$ fragment (calculated charge −0.39) of the previously reported cluster $[Mo_2(CO)_8(\mu\text{-dppm})(\mu_3\text{-H})(\mu\text{-AuPPh}_3)]$.[21]

Bonding in and Attachment of a Proton to $[Mn_3(CO)_{12}(\mu\text{-HgX})]^{2-}$. The orbital interaction of the $[HgCl]^+$ fragment with the asymmetric Mn_3 core is straightforward (Figure 5): two empty lobes of Hg–Cl of a_1 and b_1 symmetries, interact with those occupied orbitals of Mn_3 having the appropriate symmetry and topology, **G**-2a_1 and **G**-b_1, respectively. The outcome is the formation of two

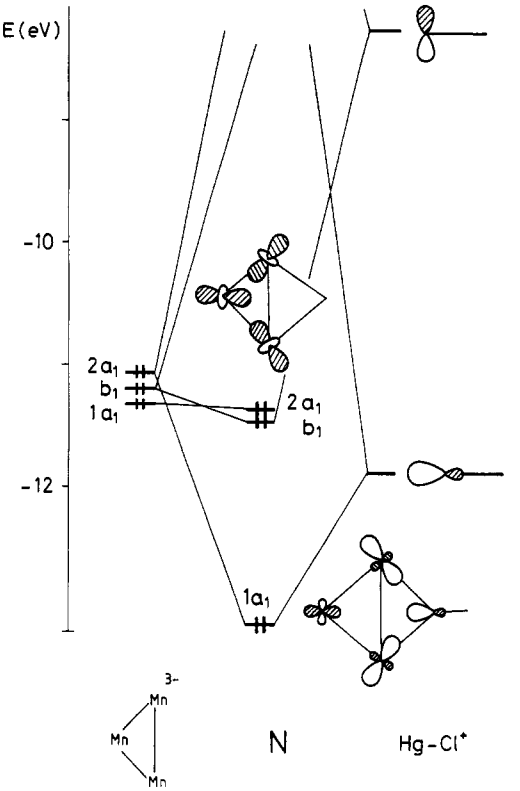

Figure 5. Diagram for the orbital interaction between the $[Mn_3(CO)_{12}]^{3-}$ cluster and a $HgCl^+$ fragment to give the model cluster $[Mn_3(CO)_{12}(\mu\text{-HgCl})]^{2-}$ (**N**).

Mn–Hg bonding MO's, mostly at the expense of electron density associated with the Mn–Mn bond of the long edge.

Let us now address the question of where in the $[Mn_3(CO)_{12}(\mu\text{-HgX})]^{2-}$ cluster is a H^+ ion more likely to be located. We have already ruled out a bridging position at one of the free edges (see discussion above). Also out-of-plane geometries are discarded given that the maximum electron density of the frontier orbitals is located in the plane of the Mn_3Hg skeleton. Calculations indeed indicate that moving the hydrogen atom out of the skeletal plane is destabilizing. A look at the frontier orbitals of **N** (Figure 5) tells us that a good interaction with the 1s orbital of H can be obtained in the middle of the Mn_3 and Mn_2Hg triangles, by using the **N**-1a_1 or **N**-2a_1 orbitals, respectively. The overlap integrals between the hydrogen 1s orbital and the corresponding fragment orbitals, **N**-1a_1 or **N**-2a_1, are quite similar, and although the Mn_3 position is computationally more stable by 0.6 eV, we cannot provide a simple explanation for such an energy difference; in this case, the Mn–H distances would be about 1.74 Å.

The calculated net charges of the hydrogen atom, obtained through a Mulliken population analysis, are −0.22 at the center of Mn_3 and −0.04 at the center of the Mn_2Hg triangle. Thus, in the former geometry the hydrogen atom has a clearer hydride character, similar to that calculated for the $[Mn_3(\mu\text{-H})(CO)_{12}]^{2-}$ (−0.20 for **E**, −0.15 for **F**) and $[Mn_3(\mu_2\text{-H})_3(CO)_{12}]$ (**L**) clusters (−0.21). If one relates the calculated charge at the hydrido ligand with its ^1H NMR chemical shift, we should conclude that the NMR of $[Mn_3(CO)_{12}(\mu_3\text{-H})(\mu\text{-Hg}\{Mo(CO)_3Cp\})]^-$ is consistent with the position of the hydride in the middle of the Mn_3 triangle given moreover the lack of Hg satellites in the hydride signal. A comparison of the signal observed in this cluster (−21.5 ppm) with that reported for the starting anion $[Mn_3(CO)_{12}(\mu\text{-H})]^-$ (−22.5 ppm)[14] is not conclusive

(21) Ferrer, M.; Reina, R.; Rossell, O.; Seco, M.; Alvarez, S.; Ruiz, E.; Pellinghelli, M. A.; Tiripicchio, A. *Organometallics* **1992**, *11*, 3753.

Table 2. Summary of Crystallographic Data for Complex 1a

mol formula	$[C_{24}H_{20}P][C_{20}H_6HgMn_3MoO_{15}]$
mol wt	1287.00
cryst syst	triclinic
space group	$P\bar{1}$
a, Å	12.511(8)
b, Å	13.604(9)
c, Å	15.200(8)
α, deg	74.20(2)
β, deg	70.08(2)
γ, deg	88.74(2)
V, Å^3	2333(3)
Z	2
D_{calcd}, g cm^{-3}	1.832
$F(000)$	1244
μ(Mo Kα), cm^{-1}	44.30
R	0.0436
R_w	0.0601

since in this complex the hydride could not be structurally characterized. However, our experience with EH calculations suggests that quantitative interpretations of the calculated charges must be taken cautiously, the above qualitative MO analysis indicates that the hydrogen atom should be located inside the Mn_3Hg rhombus, probably at its Mn_3 part, although other positions in the c---c' region in **N** cannot be ruled out, including dynamic behavior akin to that observed[22] for $[Ru_3(\mu\text{-}H)(CO)_6(\mu\text{-}dppm)_3]^+$.

Experimental Section

All manipulations were performed under an atmosphere of prepurified N_2 with use of standard Schlenk techniques, and all solvents were distilled from appropriate drying agents. Elemental analyses of C and H were carried out at the Institut de Bio-Orgànica de Barcelona. Infrared spectra were recorded in THF solutions on a FT-IR 520 Nicolet spectrophotometer. ^1H and $^{31}P\{^1H\}$ NMR spectra were obtained on a Bruker WP 80SY spectrometer. FABS(-) spectra were recorded in a Auto SPEC U, Cs^+, 30 kv, NBA matrix. The compounds $(PPh_4)_2[Mn_3(CO)_{12}(\mu\text{-}H)]$,[14] ClHg(m) (m = $Mo(CO)_3Cp$, $W(CO)_3Cp$, $Co(CO)_4$, $Mn(CO)_5$, $Fe(CO)_2Cp$),[4a] ClHgR (R = C_6Cl_5, 2,3,4,6-C_6HCl_4, 2,3,4,5-C_6HCl_4, 2,4,6-$C_6H_2Cl_3$, Ph)[23] and $[Pt(C_2H_4)(PPh_3)_2]$[24] were prepared by procedures described previously.

Synthesis of $(PPh_4)[Mn_3(CO)_{12}(\mu_3\text{-}H)(\mu\text{-}Hg(m))]$ (m = $Mo(CO)_3Cp$ (1a), $W(CO)_3Cp$ (1b), $Mn(CO)_5$ (1c), $Co(CO)_4$ (1d), $Fe(CO)_2Cp$ (1e)). Details of the synthesis of **1a** apply also to **1b–e**. To a THF (70-mL) suspension of $(PPh_4)_2[Mn_3(CO)_{12}(\mu\text{-}H)]$ (1.00 g, 0.85 mmol) was added 0.41 g of $ClHgMo(CO)_3Cp$ (0.85 mmol) at --15 °C. The mixture rapidly became dark green, and after being stirred for 30 min at this temperature, the resulting solution was filtered and concentrated to dryness. The solid was dissolved in acetone (20 mL) (filtered again if necessary), and methanol (50 mL) was added. On cooling overnight, analytically pure compound as dark green crystals was precipitated: yield 0.52 g (48%); IR (THF, cm^{-1}) ν(CO) stretch 2064 (m), 2009 (s), 1999 (s), 1983 (vs), 1957 (s), 1946 (s), 1909 (m), 1889 (m), 1868 (m); ^1H NMR (240 K, acetone-d_6, δ (ppm)) 5.7 (s, 5H, Cp), -21.5 (s, 1H, μ-H). Anal. Calcd for $(PPh_4)[Mn_3(CO)_{12}(\mu\text{-}H)(\mu\text{-}Hg\{Mo(CO)_3Cp\})]$: C, 41.04; H, 2.02. Found: C, 41.01; H, 2.09. FABS (M$^-$) Calcd: m/z 947.3. Found: m/z 947. For complex **1b**: yield 31%; IR (THF, cm^{-1}) ν(CO) stretch 2063 (m), 2009 (s), 1998 (s), 1982 (vs), 1955 (s), 1945 (s), 1908 (w), 1895 (w), 1881 (m), 1863 (m); ^1H NMR (240 K, acetone-d_6, δ (ppm)) 5.7 (s, 5H, Cp), -21.5 (s, 1H, μ-H). Anal. Calcd for $(PPh_4)[Mn_3(CO)_{12}(\mu\text{-}H)(\mu\text{-}Hg\{W(CO)_3Cp\})]$: C, 38.41; H, 1.89. Found: C, 38.12; H, 1.93. FABS (M$^-$) Calcd: m/z 1035.56. Found: m/z 1035. For complex **1c**: yield 25%; IR (THF, cm^{-1}) ν(CO) stretch 2049 (s), 2011 (s), 1998 (s), 1987 (s), 1973 (s), 1947 (s), 1912 (m); ^1H NMR (240 K, acetone-d_6, δ ppm)) -21.5 (s, 1H, μ-H). Anal. Calcd for $(PPh_4)[Mn_3(CO)_{12}(\mu\text{-}H)(\mu\text{-}Hg\{Mn(CO)_5\})]$:

Table 3. Fractional Atomic Coordinates (×10^4) and Isotropic Thermal Parameters (Å^2 × 10^4) with Esd's in Parentheses for the Non-Hydrogen Atoms of 1a

atom	x/a	y/b	z/c	U^a
		Anion		
Hg	3397.0(2)	2247.6(2)	3196.3(2)	483(1)
Mo	3283.3(4)	183.1(4)	3257.1(4)	428(2)
Mn(1)	4301.0(8)	3743.8(6)	3646.4(6)	437(3)
Mn(2)	2227.1(8)	3937.2(7)	2905.0(7)	493(4)
Mn(3)	3219.6(9)	5681.3(7)	3256.5(7)	535(4)
O(1)	5797(5)	807(7)	2952(6)	1173(45)
O(2)	3067(5)	1438(5)	1275(4)	770(26)
O(3)	4625(7)	-1111(5)	1892(5)	1050(37)
O(4)	5890(4)	5036(4)	3985(4)	711(24)
O(5)	5453(8)	1967(5)	4383(6)	1213(51)
O(6)	2699(6)	3227(5)	5703(4)	916(29)
O(7)	5951(5)	4161(5)	1617(4)	915(30)
O(8)	752(7)	5536(5)	2378(7)	1294(54)
O(9)	921(6)	2421(5)	2528(6)	1027(40)
O(10)	589(6)	3190(6)	4951(5)	1050(34)
O(11)	3754(8)	4434(8)	824(5)	1344(49)
O(12)	1886(7)	7354(5)	2594(6)	1063(40)
O(13)	4565(8)	6955(5)	3849(7)	1181(50)
O(14)	1514(8)	5270(7)	5252(5)	1265(44)
O(15)	4912(6)	6311(5)	1249(5)	1004(31)
C(1)	4868(6)	630(7)	3048(6)	701(36)
C(2)	3164(6)	1001(5)	2018(5)	560(27)
C(3)	4119(7)	-639(6)	2390(5)	668(32)
C(4)	5212(6)	4576(5)	3869(5)	529(25)
C(5)	5005(8)	2645(6)	4046(7)	740(40)
C(6)	3277(7)	3449(5)	4909(5)	585(28)
C(7)	5295(6)	4003(5)	2384(5)	558(29)
C(8)	1369(8)	4968(7)	2578(8)	863(48)
C(9)	1470(7)	3010(6)	2653(6)	698(36)
C(10)	1256(7)	3502(6)	4167(6)	688(35)
C(11)	3191(7)	4262(7)	1636(6)	738(37)
C(12)	2387(8)	6680(6)	2861(7)	770(39)
C(13)	4054(9)	6446(6)	3606(7)	779(42)
C(14)	2144(9)	5370(7)	4503(7)	870(43)
C(15)	4276(6)	6040(5)	2014(6)	635(30)
C(16)	1345(6)	-162(7)	4192(5)	677(32)
C(17)	1840(7)	279(7)	4695(5)	731(34)
C(18)	2665(7)	-387(6)	4960(5)	698(34)
C(19)	2605(8)	-1223(6)	4619(5)	738(35)
C(20)	1803(7)	-1078(6)	4146(6)	739(34)
		Cation		
P	-881(1)	1874(1)	936(1)	415(5)
C(21)	-670(5)	672(4)	1689(4)	463(22)
C(22)	-1634(6)	76(5)	2395(5)	597(26)
C(23)	-1495(7)	-834(5)	3009(5)	674(29)
C(24)	-420(8)	-1168(5)	2909(5)	721(36)
C(25)	519(7)	-585(5)	2215(5)	689(33)
C(26)	403(5)	342(5)	1610(4)	524(24)
C(27)	-1172(5)	2823(4)	1584(4)	425(20)
C(28)	-959(7)	3843(5)	1073(5)	705(32)
C(29)	-1172(9)	4589(5)	1562(6)	909(43)
C(30)	-1607(7)	4331(6)	2539(5)	698(32)
C(31)	-1856(7)	3319(6)	3067(5)	732(33)
C(32)	-1637(6)	2569(5)	2586(5)	614(27)
C(33)	389(5)	2320(4)	-106(4)	488(22)
C(34)	1363(6)	2592(6)	28(5)	738(31)
C(35)	2358(7)	2902(7)	-755(7)	977(44)
C(36)	2386(8)	2985(7)	-1670(8)	998(46)
C(37)	1402(9)	2766(7)	-1824(6)	950(44)
C(38)	400(7)	2415(5)	-1042(5)	690(30)
C(39)	-2060(5)	1675(5)	572(4)	513(24)
C(40)	-2863(7)	2399(7)	556(6)	717(35)
C(41)	-3779(8)	2230(9)	281(7)	978(51)
C(42)	-3894(8)	1366(9)	41(7)	961(52)
C(43)	-3143(8)	635(9)	66(7)	985(51)
C(44)	-2198(6)	786(6)	337(6)	693(33)

[a] Equivalent isotropic U defined as one-third of the trace of the orthogonalized U_{ij} tensor.

(22) Mirza, H. A.; Vittal, J. J.; Puddephatt, R. J. *Inorg. Chem.* **1993**, *32*, 1327.
(23) Crespo, M.; Rossell, O.; Sales, J.; Seco, M. *Polyhedron* **1982**, *1*, 243.
(24) Nagel, U. *Chem. Ber.* **1982**, *115*, 1998.

C, 39.80; H, 1.70. Found: C, 39.57; H, 1.63. FABS (M^-) Calcd: m/z 897.34. Found: m/z 899. For complex **1d**: yield 37%; IR (THF, cm^{-1}) ν(CO) stretch 2047 (s), 2018 (s), 2005 (s), 1990 (vs), 1972 (s), 1951 (s), 1920 (m); ^1H NMR (240 K, acetone-d_6, δ (ppm)) −21.1 (s, 1H, μ-H). Anal. Calcd for $(PPh_4)[Mn_3(CO)_{12}(\mu\text{-H})(\mu\text{-Hg}\{Co(CO)_4\})]$: C, 39.59; H, 1.73. Found: C, 39.71; H, 1.78. FABS (M^-) Calcd: m/z 873.34. Found: m/z 875. For complex **1e**: yield 30%; IR (THF, cm^{-1}) ν(CO) stretch 2061 (m), 2005 (s), 1991 (vs), 1979 (vs), 1956 (s), 1942 (s), 1923 (s); ^1H NMR (240 K, acetone-d_6, δ (ppm)) 5.0 (s, 5H, Cp), −21.5 (s, 1H, μ-H). Anal. Calcd for $(PPh_4)[Mn_3(CO)_{12}(\mu\text{-H})(\mu\text{-Hg}\{Fe(CO)_2Cp\}]$: C, 42.37; H, 2.13. Found: C, 42.19; H, 2.13. FABS (M^-) Calcd: m/z 879.25. Found: m/z 880.

Synthesis of $(PPh_4)_2[\{Mn_3(CO)_{12}(\mu_3\text{-H})\}_2(\mu_4\text{-Hg})]$ (2). This complex was similarly obtained from 1.86 g (1.58 mmol) of $(PPh_4)_2[Mn_3(CO)_{12}(\mu\text{-H})]$ and 0.79 mmol of $Hg(NO_3)_2$ in acetone at −10 °C. After filtration, the green solution was concentrated to dryness, and the solid, dissolved in the minimum quantity of acetone and hexane, was added dropwise. The dark green crystals obtained on cooling were filtered off and dried. Yield: 0.38 g (26%). IR (THF, cm^{-1}): ν(CO) stretch 2045 (m), 2006 (s) 1989 (vs), 1954 (s), 1935 (s), 1924 (m), 1899 (m). ^1H NMR (25 °C, acetone-d_6, δ (ppm)): −21.1. Anal. Calcd for $(PPh_4)_2[\{Mn_3(CO)_{12}(\mu_3\text{-H})\}_2(\mu_4\text{-Hg})]$: C, 45.9; H, 2.23. Found: C, 46.26; H, 2.35. FAB (M^-) Calcd: m/z 1204.2. Found: m/z 1205.

Synthesis of $(PPh_4)[Mn_3(CO)_{12}(\mu_3\text{-H})(\mu\text{-HgR})]$ (R = C_6Cl_5 (3a), 2,3,4,6-C_6HCl_4 (3b), 2,4,6-$C_6H_2Cl_3$ (3c). Details of the synthesis of **3a** also apply to **3b,c**. To a THF (70-mL) suspension of $(PPh_4)_2[Mn_3(CO)_{12}(\mu\text{-H})]$ (1.75 g, 1.48 mmol) was added 0.72 g (1.48 mmol) of $ClHg(C_6Cl_5)$ at −15 °C. After 15 min of stirring, the resulting solution was filtered and concentrated to dryness and the solid was dissolved in the minimum quantity of methanol. On overnight cooling, green crystals were formed. Yield: 1.24 g (65%). IR (THF, cm^{-1}): ν(CO) stretch 2068 (s), 2015 (vs), 2002 (vs), 1986 (vs), 1964 (sh), 1949 (vs), 1939 (sh), 1916 (s), 1902 (sh). ^1H NMR (25 °C, acetone-d_6, δ (ppm)): −21.5. Anal. Calcd for $(PPh_4)[Mn_3(CO)_{12}(\mu\text{-H})(\mu\text{-Hg}\{C_6Cl_5\})]$ (**3a**): C, 39.05; H, 1.63. Found: C, 38.91; H, 1.59. For complex **3b**: yield 0.34 g (39%); IR (THF, cm^{-1}) ν(CO) stretch 2067 (s), 2014 (vs), 2001 (vs), 1984 (vs), 1963 (sh), 1948 (s), 1938 (sh), 1915 (s), 1902 (sh); ^1H NMR (25 °C, acetone-d_6, δ (ppm)) −21.5. Anal. Calcd for $(PPh_4)[Mn_3(CO)_{12}(\mu\text{-H})(\mu\text{-Hg}\{2,3,4,6\text{-}C_6HCl_4\})]$: C, 40.14; H, 1.75. Found: C, 39.95; H, 1.78. For complex **3c**: yield 0.11 g (40%); IR (THF, cm^{-1}) ν(CO) stretch 2067 (s), 2014 (vs), 2001 (vs), 1984 (vs), 1962 (sh), 1947 (s), 1937 (sh), 1914 (s), 1900 (sh); ^1H NMR (25 °C, acetone-d_6, δ (ppm)) −21.5. Anal. Calcd for $(PPh_4)[Mn_3(CO)_{12}(\mu\text{-H})(\mu\text{-Hg}\{2,4,6\text{-}C_6H_2Cl_3\})]$: C, 41.28; H, 1.88. Found: C, 41.17; H, 1.81.

Synthesis of $(PPh_4)[Mn_3(CO)_{12}(\mu_3\text{-H})(\mu\text{-Hg}\{Pt(C_6Cl_5)(PPh_3)_2\})]$ (4). $[Pt(C_2H_4)(PPh_3)_2]$ (0.19 g, 0.25 mmol) was added to a suspension of $(PPh_4)[Mn_3(CO)_{12}(\mu\text{-H})\{\mu\text{-Hg}(C_6Cl_5)\}]$ (0.33 g, 0.25 mmol) in 40 mL of THF at 40 °C. When the reaction was completed (about 1 h, IR monitoring), the green solution was evaporated to dryness and the residue was recrystallized from acetone/methanol to give a green powder of **4**. Yield: 0.14 g (25%). IR (THF, cm^{-1}): ν(CO) stretch 2055 (s), 2001 (s), 1985 (vs), 1977 (vs), 1951 (s), 1932 (s), 1899 (m). ^1H NMR (25 °C, acetone-d_6, δ (ppm)): −21.7. Anal. Calcd for $(PPh_4)[Mn_3(CO)_{12}(\mu\text{-H})(\mu\text{-Hg}\{Pt(C_6Cl_5)(PPh_3)_2\})]$: C, 42.99; H, 2.5. Found: C, 41.83; H, 2.20.

X-ray Data Collection, Structure Determination, and Refinement for $(PPh_4)[Mn_3(CO)_{12}(\mu_3\text{-H})(\mu\text{-Hg}\{Mo(CO)_3Cp\})]$ (1a). A single crystal of ca. 0.24 × 0.27 × 0.35 mm was selected and used for data collection. The crystallographic data are summarized in Table 2. Data were collected at room temperature on a Siemens AED diffractometer, using the niobium-filtered Mo Kα radiation ($\bar{\lambda}$ = 0.710 73 Å) and the $\theta/2\theta$ scan type. The reflections were collected with a variable scan speed of 3–12° min^{-1} and a scan width from (θ–0.60)° to (θ + 0.60 + 0.346 tan θ)°. Of 11 055 unique reflections, with θ in the range 3–28°, 7351 with $I \geq 2\sigma(I)$ were used for the analysis. One standard reflection was monitored every 50 measurements; no significant decay was noticed over the time of data collection. The individual profiles have been analyzed following Lehmann and Larsen.[25] Intensities were corrected for Lorentz and polarization effects. A correction for absorption was applied (maximum and minimum values for the transmission factors were 1.342 and 0.817).[26]

The structure was solved by direct and Fourier methods and refined first by full-matrix least-squares methods with isotropic thermal parameters and then by blocked full-matrix least-squares methods with anisotropic thermal parameters for all non-hydrogen atoms. All hydrogen atoms, excepting the hydride which could not be located unambiguously, were placed at their geometrically calculated positions (C–H = 0.96 Å) and refined "riding" on the corresponding carbon atoms. The final cycles of refinement were carried out on the basis of 588 variables; after the last cycles, no parameters shifted by more than 0.68 esd. The biggest remaining peak (close to the mercury atom) in the final difference map was equivalent to about 1.82 e/Å^3. In the final cycles of refinement a weighting scheme, $w = K[\sigma^2(F_0) + gF_0^2]^{-1}$ was used; at convergence the K and g values were 0.695 and 0.0086, respectively. The analytical scattering factors, corrected for the real and imaginary parts of anomalous dispersions, were taken from ref 27. All calculations were carried out on the GOULD POWERNODE 6040 and ENCORE 91 computers of the "Centro di Studio per la Strutturistica Diffrattometrica" del CNR, Parma, Italy, using the SHELX-86 and SHELXS-86 systems of crystallographic computer programs.[28] The final atomic coordinates for the non-hydrogen atoms are given in Table 3. The atomic coordinates of the hydrogen atoms are given in Table SI, and the thermal parameters, in Tables SII.

Acknowledgment. Financial support for this work was generously given by the DGICYT (Spain), through Grants PB90-0055-C02-01 (experimental work) and PB92-0655-C02-01 (theoretical work) and the Italian Ministero della Università e della Ricerca Scientifica e Tecnologica. We thank X. Huguet and J. Caixac for facilities in recording the FAB(−) spectra. G.S. in indebted to a scholarship from the Ministerio de Educación y Ciencia.

Supplementary Material Available: Tables of hydrogen atom coordinates (Table SI), anisotropic thermal parameters for the non-hydrogen atoms (Table SII), and bond distances and angles (Table SIII) (6 pages). Ordering information is given on any current masthead page.

OM9306483

(25) Lehmann, M. S.; Larsen, F. K. *Acta Crystallogr., Sect. A* **1974**, *30*, 580.
(26) Walker, N.; Stuart, D. *Acta Crystallogr., Sect. A* **1983**, *39*, 158. Ugozzoli, F. *Comput. Chem.* **1987**, *11*, 109.
(27) *International Tables for X-Ray Crystallography*; Kynock *Press*: Birmingham, England, 1974; Vol. IV.
(28) Sheldrick, G. M. *SHELX*-76 Program for crystal structure determination. University of Cambridge, England, 1976; SHELXS-86 Program for the solution of crystal structures. University of Göttingen, 1986.